

## Binding-Energy Systematics of $0^+$ , $2^+$ , $3^-$ , and $4^-$ , $T = 0$ States of Even–Even Self-Conjugate Nuclides from $^{16}\text{O}$ to $^{40}\text{Ca}$

Friedrich EVERLING<sup>1,2\*</sup>

<sup>1</sup>Department of Physics, North Carolina State University, Raleigh, NC 27695-8282, U.S.A.

<sup>2</sup>Triangle Universities Nuclear Laboratory, Durham, NC 27708-0308, U.S.A.

(Received May 29, 2006; accepted September 26, 2006; published November 27, 2006)

Binding energies of self-conjugate even–even nuclides are plotted as  $-B^* + (9.5 \text{ MeV}) \cdot A$  versus mass number  $A$ , where  $B^*$  is the binding energy of ground states and levels. A diagram from  $A = 0$  to 76 mainly for ground states shows a subshell systematics. In a diagram from  $A = 16$  to 40, established and hypothetical  $0^+$  levels are shown; 24 states of supposed  $1d_{5/2}$ ,  $2s_{1/2}$ , and  $1d_{3/2}$  subshell occupations are connected by almost linear trends. Surprisingly, early insufficient measurements at  $E_x = 0.65 \text{ MeV}$  in  $^{20}\text{Ne}$  and 0.5 (and 0.43) MeV in  $^{32}\text{S}$  fit the trends. A diagram for the  $0^+$ ,  $2^+$ ,  $4^+$ , and  $6^+$  band from  $^{16}\text{O}$  to  $^{28}\text{Si}$  suggests the  $0^+$  head in  $^{20}\text{Ne}$  to be at 0.65 MeV. A systematics of  $2^+$  states supports both levels. A plot of  $3^-$  and  $4^-$  states contains two pairs of nearly parallel and linear 3-point trends. A table suggests a total of 18 important experimental investigations.

KEYWORDS: level energies,  $J^\pi$ , nuclear binding-energy systematics

DOI: [10.1143/JPSJ.75.124201](https://doi.org/10.1143/JPSJ.75.124201)

### 1. Introduction

Ground-state binding energies of nuclides together with their level schemes provide direct and reliable information on nuclear structure which is governed by the Shell Model with its magic numbers. It is not known how the subshells determine the nuclear structure. This work investigates an empirical systematics according to approximately pure subshell states.

The work specializes on  $N = Z$  nuclides with even neutron number  $N$  and proton number  $Z$ . After an overview for the ground states from mass number  $A = 0$  to 76, the range  $A = 16$  to 40 is considered involving the subshells  $1d_{5/2}$ ,  $2s_{1/2}$ , and  $1d_{3/2}$ . The filling of these subshells in this order leads from the first excited state of  $^{16}\text{O}$  over  $^{28}\text{Si}$  and  $^{32}\text{S}$  to  $^{40}\text{Ca}$ . Other sequences and partial shell occupation should involve also other excited states with  $J^\pi = 0^+$ .

The method described is also used to display the rotational bands  $0^+$ ,  $2^+$ ,  $4^+$ , and  $6^+$ , and yields a much more elucidating plot than the customary one of excitation energies with respect to the supposed  $0^+$  band-head. Also the application to higher  $2^+$  levels is done below.

Furthermore, a diagram for the  $3^-$  and  $4^-$  levels is given as an example for almost linear relations for spins other than  $0^+$  and  $2^+$ .

Traditionally, nuclidic *ground-state binding energies* are obtained from atomic mass tables. Continuing efforts for many decades by Mattauch, Wapstra and others, e.g., refs. 1 and 2, have provided least-squares-adjusted atomic masses together with  $Q$ -values. Decades ago, the binding energies were plotted for isobaric chains and in the form of  $B/A$  for constant neutron excess, or as differences such as separation energies to circumvent the steep increase of  $B$  with the mass number.<sup>3)</sup> On the other hand, *level schemes* are usually displayed in *isobaric chains*.

However, a diagram is needed which combines the level schemes with the binding energies of the ground states. The first comprehensive diagram of this kind was published in 1958;<sup>4)</sup> the nuclides selected had *constant neutron excess*. The method visualised the gain in binding energy upon addition of the constituents of an  $\alpha$ -particle, 2 protons and 2 neutrons.

The search for smooth trends within subshells of the Shell Model requires that the spin  $J^\pi$ , angular momentum quantum number and parity, be the same for each member of the sequence. Particularly at shell closures, a trend may proceed from excited states to a ground state or *vice versa*. The negative value of the binding energy of an excited state,  $-B^*$ , is considered, where the ground state appears as a special case. Due to the minus sign, increasing excitation energy means going up in the diagram as is customary in level schemes, because the nuclear binding energy is reduced with increasing excitation. The trends thus obtained are more meaningful than those of the ground states alone and those of a selected  $J^\pi$  for normalized ground states. This is also true for the even–even nuclei (even  $Z$  and even  $N$ ) of this paper, where  $0^+$  levels can be connected with  $0^+$  ground states.

In order to compensate for the steep decrease of  $-B^*$  with the mass number, a linear function of the mass number  $A$  was added, so that the ordinate becomes  $-B^* + C \cdot A$ , where  $C$  is a constant. In contrast to a plot of  $B/A$ , linear relationships are preserved. Also  $\Delta + C \cdot A$  was plotted,<sup>5,6)</sup> where  $\Delta$  was defined as the mass excess for the ground state and excited states (inadvertently, the unit MeV of  $C$  was omitted in the diagrams).

More common are diagrams of *differences of binding energies*, such as separation energies and beta-decay energies. Then the compensation term is not needed; on the other hand, important information is lost for algebraic reasons. The first examples of diagrams including excited states were separation energies,<sup>7)</sup> beta-decay energies,<sup>8)</sup> and Coulomb-energy differences of mirror nuclei.<sup>9)</sup> In each case, nearly straight trends could be located.

\*The affiliation given is an early one essential for the findings reported here in detail for the first time. Present address: Ringheide 24 f, 21149 Hamburg, Germany. E-mail: everlingf@aol.com

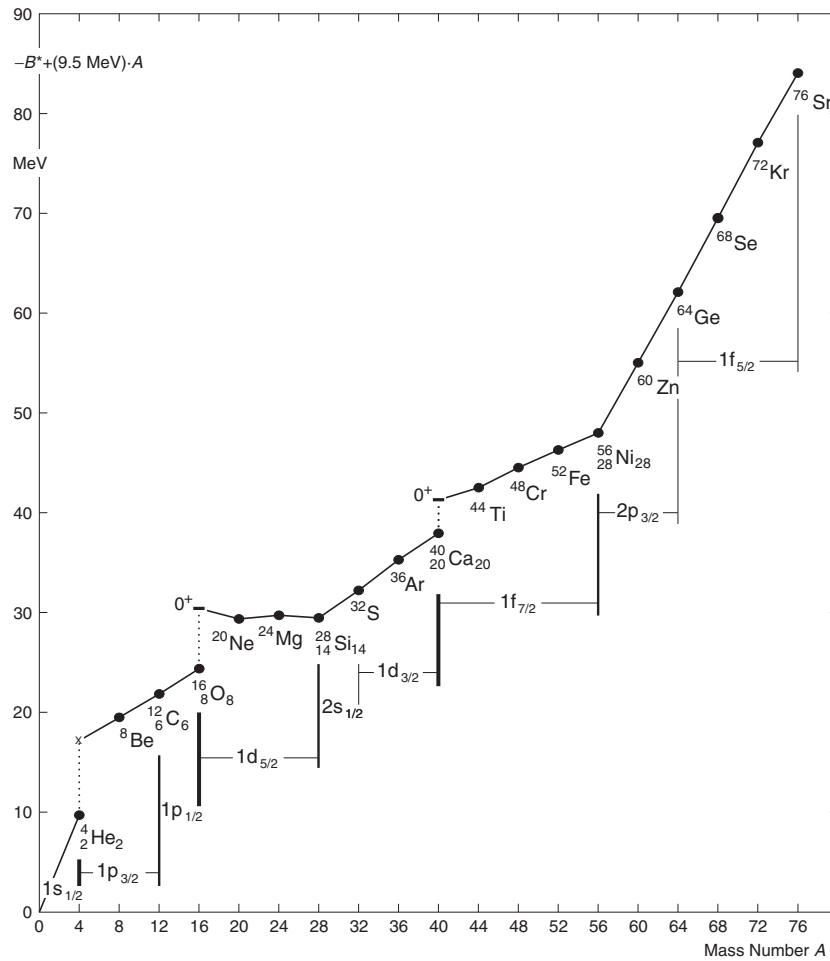


Fig. 1. Nuclear binding energy  $B^*$ , itself a positive quantity, plotted negative with a linear term  $(9.5 \text{ MeV}) \cdot A$  added, for even–even self-conjugate nuclides. The star (\*) on  $B$  is used because two first excited states (dashes) are included. The cross (x) at  ${}^4\text{He}$  marks the prolongation from  ${}^{12}\text{C}$  over  ${}^8\text{Be}$  only. Uncertainties are  $\leq 40 \text{ keV}$ . Ground state spins  $0^+$  and  $T = 0$  are omitted. Subshells of the Shell Model are indicated. Vertical dotted lines indicate steps of 7.46, 6.05, and 3.35 MeV.

As regards the trends in diagrams for ground states and excited states, it was noticed<sup>5)</sup> that *steps* of 6.05 MeV occur in the mass excess at  ${}^{16}\text{O}$  for self-conjugate nuclides and in the vicinity of  ${}^{16}\text{O}$  for other chains of constant neutron excess. The steps were interpreted as a *rearrangement* of the nucleons before the  $1d_{5/2}$  subshell can be accommodated in a regular way. The same was shown in binding-energy diagrams<sup>10)</sup> instead of mass excess diagrams, and the phenomenon was also investigated for the vicinity of  ${}^{40}\text{Ca}$ .<sup>6)</sup>

## 2. General Remarks on the Binding-Energy Diagrams Shown

The nuclear binding energy, also known as “total nuclear binding energy” to avoid confusion with quantities properly called “separation energy”, is defined as  $B(Z, N) = N \cdot M({}^1_0\text{n}) + Z \cdot M({}^1_1\text{H}) - M(Z, N)$ , where  $Z$  is the proton number,  $N$  the neutron number, and  $M$  the atomic mass. This is a good approximation with respect to the electron binding energies. The substitution  $M = A + m$ , where  $A$  is the mass number and  $m$  the atomic mass excess, leads to  $B(Z, N) = N \cdot m({}^1_0\text{n}) + Z \cdot m({}^1_1\text{H}) - m(Z, N)$  because the mass number cancels. The word “atomic” in “atomic mass” is often replaced by “nuclidic”. The positive quantity  $B$  refers to the ground state, while  $B^* = B - E_x$  is the binding energy for excited states with the ground state as a special case where

$E_x = 0$ ;  $E_x$  is the excitation energy.

Values of the binding energies were taken from the 2003 Atomic Mass Table.<sup>11)</sup> Levels were taken from the well-known compilations for mass numbers  $A = 12$ ,<sup>12)</sup>  $A = 16$ – $17$ ,<sup>13)</sup>  $A = 20$ ,<sup>14)</sup>  $A = 21$ – $39$ ,<sup>15)</sup> and  $A = 40$ .<sup>16)</sup>

## 3. Steps at the Beginning of Certain Subshells in a Diagram from $A = 0$ to 76

Figure 1 shows a diagram of the self-conjugate nuclides with even proton and neutron numbers. The smooth trend in the  $1f_{7/2}$  subshell from  ${}^{40}\text{Ca}$  to  ${}^{56}\text{Ni}$  does not begin at the ground state; it begins at or near the 3.353-MeV,  $0^+$  level of  ${}^{40}\text{Ca}$ . Correspondingly, the trend of the  $1d_{5/2}$  subshell leading to  ${}^{28}\text{Si}$  starts at the 6.049-MeV,  $0^+$  level of  ${}^{16}\text{O}$ , doubly magic as  ${}^{40}\text{Ca}$ .

At  $A = 4, 16, \text{ and } 40$ , the Shell Model would suggest a break rather than a step as is the case at  ${}^{28}\text{Si}$  and  ${}^{56}\text{Ni}$ . It should be noted that steps principally occur in diagrams of the separation energy only. The well-known schematic representation of the level sequence in the spherically symmetric potential of the isotropic harmonic oscillator does not mean that there are steps also in the binding energy as a function of mass number.

At  $A = 4$  there is no  $0^+$  level at 7.458 MeV, where a cross is drawn as a reference point.

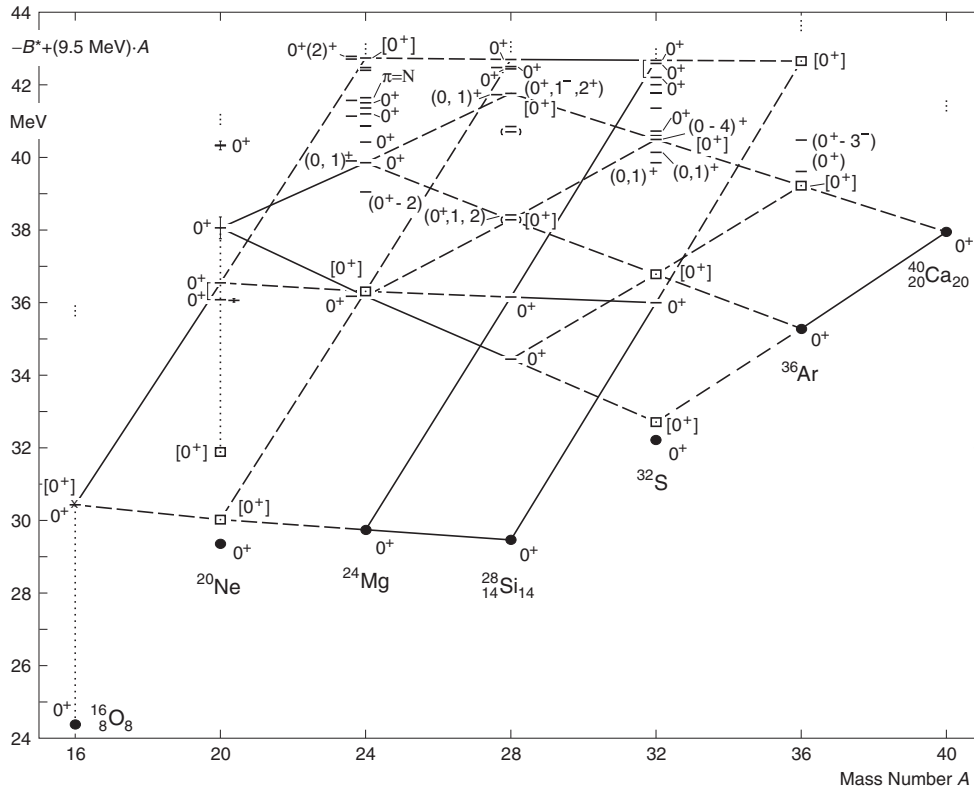


Fig. 2. Binding-energy diagram of self-conjugate even-even nuclides as in Fig. 1, but limited to  $A = 16$  to  $40$  and with established, possible, and complementary  $0^+$  levels added. A reference point (cross) at  $^{16}\text{O}$  is also included (see Fig. 8). All levels with spins other than  $0^+$  are omitted. If  $J^\pi$  is not given, it is not known.  $T = 0$  on the spins  $0^+$  is omitted. Uncertainties are  $\leq 10$  keV unless indicated.

**Explanation of Symbols**

- Ground state
  - Excited state
  - (Full line) Attachment of 2 protons and 2 neutrons
  - - - (Dashed line) Connection involving a complementary level, reference point, or uncertain level (in parentheses)
  - ..... (Dotted line) Extension into a region of high level density and insufficient data (Figs. 10 and 11)
  - 3 dots Starting at this excitation energy, all levels are omitted.
  - (Square) Complementary level suggested by nearly straight trends. It does not necessarily exist at this position, but may be forbidden by unknown selection rules. In this case it serves as a reference point.
  - × Reference point, probably forbidden by unknown selection rules
  - ( ) Indication of doubt for a level or  $J^\pi$
  - [ ] Expected excitation energy of a complementary level, or expected  $J^\pi$
  - Dotted line Rearrangement of 6.05 MeV, starting at  $^{16}\text{O}$  g.s. and  $^{20}\text{Ne}$  (2.53 MeV) (vertical)
  - [ Possible pair of  $0^+$  levels in analogy to the pair of a low-lying complementary state and the ground state in  $^{20}\text{Ne}$  and  $^{32}\text{S}$
  - $\pi = N$  Parity is "normal", i.e.  $J^\pi = 0^+, 1^-, 2^+, 3^-, \dots$
  - $\uparrow\downarrow$  or  $\uparrow\uparrow$  Relative spin orientation for the odd proton and neutron (Fig. 13 only)
- The  $^{24}\text{Mg}$  13.041-MeV,  $0^+(2^+)$  level slightly above the upper left corner of the large parallelogram has a  $T = 1$  admixture not indicated in the graph; the same is true for the  $^{28}\text{Si}$  12.3007-MeV,  $0^+(1^-, 2^+)$  level constituting the upper corner of the other parallelogram.

**4. Diagram of  $J^\pi = 0^+$  States for  $A = 16$  to  $40$**

Figure 2 is a section of Fig. 1 from  $A = 16$  to  $40$ . For each of the self-conjugate nuclides, all  $0^+$ ,  $T = 0$  levels are plotted up to the height indicated by 3 vertical dots. All levels are omitted of which the spin and parity are not  $0^+$ ,  $T = 0$ . If no assignment has been made to a level, it is included, because it may turn out to have  $0^+$ ,  $T = 0$ .

A preliminary presentation of this diagram was given in an oral contribution at a conference in the year 2000.<sup>17)</sup> The present diagram is an updated version, leading to some changes in the table of complementary levels and requirements for known levels.

The  $1d_{5/2}$  trend from Fig. 1 is drawn as a straight line between  $A = 20$  to  $28$ , raising the question of whether the ground state of  $^{20}\text{Ne}$ , 0.668 MeV below the trend, belongs to it at all.

In 1958 Morita and Takeshita<sup>18)</sup> found some indication for a level in  $^{20}\text{Ne}$  at  $0.65 \pm 0.04$  MeV (or  $0.65 \pm 0.04$  MeV in the style used here) in the  $^{19}\text{F}(d,n)^{20}\text{Ne}$  reaction. This doubtful level was not included in the table of energy levels of  $^{20}\text{Ne}$  in the compilations of Ajzenberg-Selove and the recent one of Tilley *et al.*<sup>14)</sup> because it has not been confirmed.

For an even-even nucleus it would in fact be unusual to have a  $0^+$  level close to the ground state below the first  $2^+$  level. A  $0^+$  level as a first excited state is known to exist in

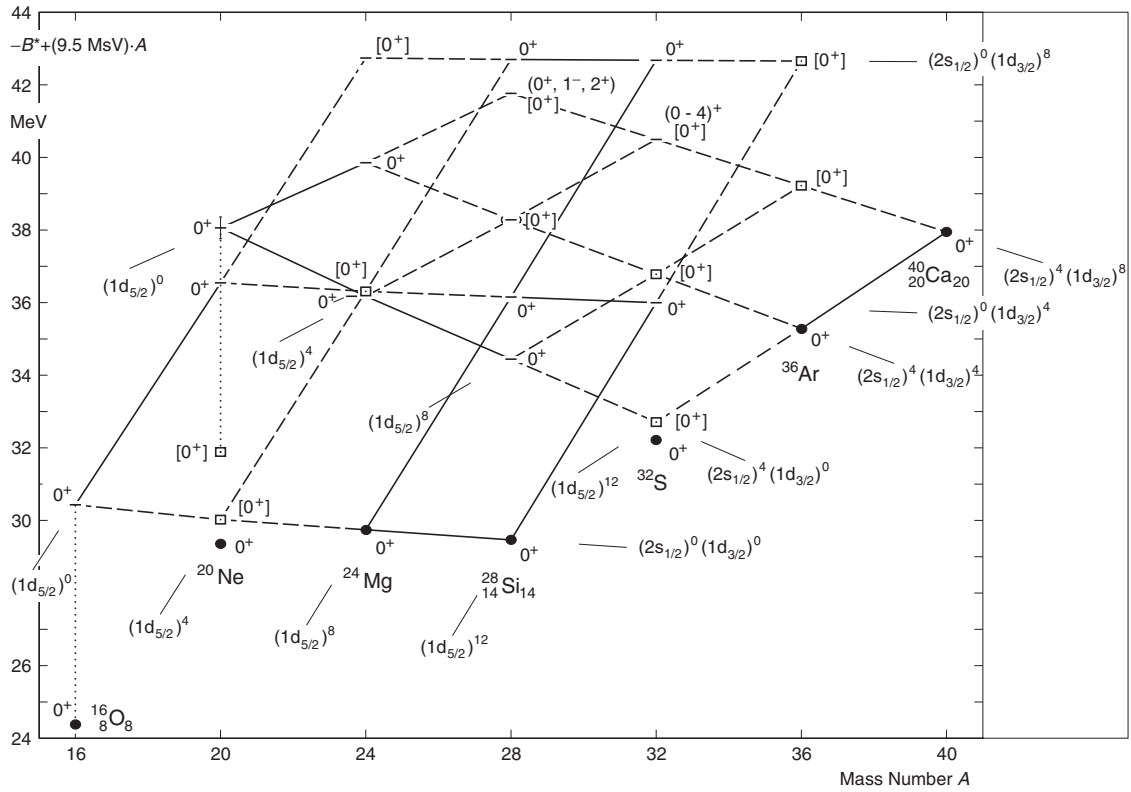


Fig. 3. Same as Fig. 2, but only levels connected by lines are shown, and Shell Model configurations are indicated. Uncertainties are  $\leq 9$  keV unless shown.

doubly magic nuclei, yet at much higher excitation energy. In the singly magic  $^{186}\text{Pb}$ , however, there are even two  $0^+$  excited states at 0.532 and 0.650 MeV, i.e., below the first  $2^+$  level, due to shape coexistence.<sup>19)</sup>

Should an *extremely weak* 0.65-MeV level in  $^{20}\text{Ne}$  actually exist and have the spin  $0^+$ , Figs. 2 and 3 suggest a configuration  $(1d_{5/2})^4$  on the trend established by the ground states of  $^{24}\text{Mg}$  and  $^{28}\text{Si}$  which are known to complete this subshell in two steps, leading via  $(1d_{5/2})^8$  to  $(1d_{5/2})^{12}$ . For the ground state of  $^{20}\text{Ne}$  the configuration would have to be different from  $(1d_{5/2})^4$ ,  $(2s_{1/2})^4$ , and  $(1d_{3/2})^4$ , because these configurations are assigned to other states. Perhaps it could be  $(1d_{5/2})^2(2s_{1/2})^2$ ,  $(1d_{5/2})^2(1d_{3/2})^2$ , or  $(2s_{1/2})^2(1d_{3/2})^2$ .

The beginning of this trend should be characterized by an empty  $1d_{5/2}$  shell. Such a state would have the same Shell-Model configuration  $(1s_{1/2})^4(1p_{3/2})^8(1p_{1/2})^4$  as the  $^{16}\text{O}$  ground state, with a rearrangement leading to shape coexistence.

Including the lowest  $1d_{5/2}$  trend just discussed, there are 14 more or less tentative trends connecting 3 or 4 points. One trend from the left to the right side ends near the ground state of  $^{32}\text{S}$ . It is interpreted as the occupation of the  $1d_{5/2}$  subshell by 0, 4, 8, and 12 nucleons in the presence of four  $2s_{1/2}$  nucleons. This trend, and the line connecting the ground states of  $^{40}\text{Ca}$  and  $^{36}\text{Ar}$ , point to a low-lying position at 0.5 MeV in  $^{32}\text{S}$ .

A level was observed by Snowdon<sup>20)</sup> in 1952 at  $0.5 \pm 0.1$  MeV and by Singh<sup>21)</sup> in 1956 at 0.43 MeV (without uncertainty information). It was not detected by Ferguson *et al.*<sup>22)</sup> in 1968 who used the same reaction  $^{31}\text{P}(d,n)^{32}\text{S}$ . Should this state exist, it is *very weakly populated* and not resolved from the ground state peak in the work of

Ferguson *et al.* In this context, it would have the configuration  $(1d_{5/2})^{12}(2s_{1/2})^4$ . The  $^{32}\text{S}$  ground state might have the configuration  $(1d_{5/2})^{12}(2s_{1/2})^2(1d_{3/2})^2$ .

The short trend from the position at 0.5 MeV in  $^{32}\text{S}$  over the ground state of  $^{36}\text{Ar}$  to  $^{40}\text{Ca}$  is interpreted as the filling of the  $1d_{3/2}$  subshell—initially empty—by 4 and 8 nucleons.

The two cases  $^{20}\text{Ne}$  and  $^{32}\text{S}$  have in common that they exceed closed-shell nuclides, the doubly-magic  $^{16}\text{O}_8$  and the doubly semi-magic  $^{28}\text{Si}_{14}$ , by 2 protons and 2 neutrons. Furthermore, both levels were obtained with the old technique of using photographic plates in 1958 ( $^{20}\text{Ne}$ )<sup>18)</sup> and in 1952<sup>20)</sup> and 1956 ( $^{32}\text{S}$ ).<sup>21)</sup>

Such levels, which complete the systematics, including those for which insufficient experimental evidence exists, are introduced here as “*complementary levels*”. Whether they exist in nature is *uncertain*. The new systematics may be governed by unknown selection rules, therefore complementary levels are *not predictions*.

The state in  $^{20}\text{Ne}$  at  $2.53 \pm 0.07$  MeV, also shown in Fig. 2 by a square, was observed but not definitely established by Morita and Takeshita<sup>18)</sup> together with the 0.65-MeV level mentioned above. It was also not confirmed and therefore omitted in the compilations. If it existed, it could be interpreted as the *unrearranged*  $^{16}\text{O}$  ground state with  $(2s_{1/2})^4$  attached, because it is situated 6.17 MeV below the 8.7-MeV,  $0^+$  level, close to the basic step size 6.049 MeV in  $^{16}\text{O}$ . The step effect mentioned is evident here too, assuming that the 2.53-MeV level exists.

The occurrence of  $0^+$  excitations of even-even nuclides in neighbouring nuclides and in their own level scheme, and as difference of states with the same spin and parity, was first reported in 1960.<sup>23)</sup> Likewise, first evidence was given in 1971<sup>24)</sup> of the fact that the spacing of the band  $0^+$ ,  $2^+$ , and

$4^+$  of the  $^{24}\text{Mg}$  core deviates only 11 and 7 keV from that of the  $1/2^+$ ,  $5/2^+$ , and  $9/2^+$  rotational band in  $^{25}\text{Mg}$ . In this case, a single  $2s_{1/2}$  neutron is the “spectator”, while in  $^{20}\text{Ne}$  four  $2s_{1/2}$  nucleons would be “spectators” in the transition from the 2.53- to the 8.7-MeV level, which do not appreciably influence the core excitation.

At  $^{20}\text{Ne}$  and  $^{32}\text{S}$  of Fig. 2, two levels are connected by a bracket, because an analogy to the complementary low-lying  $0^+$  levels and the ground states seems indicated. The same phenomenon exists for spin  $0^+$ ,  $T = 1$  in  $^{34}\text{Cl}$  and for spin  $1^+$  in  $^{18}\text{F}$ , not discussed in this publication.

Figure 3 is the same as Fig. 2, except that all levels are omitted which do not belong to the system of the two large parallelogram-like shapes and the two unrearranged states.

The 24 states on the parallelogram-like shapes are assumed to have relatively pure Shell-Model configurations  $(1d_{5/2})^i(2s_{1/2})^j(1d_{3/2})^k$  with nucleon numbers  $i = 0, 4, 8, 12$ ,  $j = 0, 4$ , and  $k = 0, 4, 8$ , where  $i + j + k = 0, 4, 8, \dots, 24$ , and  $A = 16 + i + j + k = 16, 20, 24, \dots, 40$ .

If the unrearranged states, the ground state of  $^{16}\text{O}$  and the  $^{20}\text{Ne}(2.53\text{ MeV})$  level, are included, the systematics described concerns 26 states, of which 15 are empirically established  $0^+$  states, 5 being ground states. In the remaining 11 cases the existence of a  $0^+$  level is more or less uncertain. Two of them have ambiguous spin assignments, among them  $0^+$ , and two are lacking any spin determinations so far. Seven levels are complementary, of which 3 coincide with early insufficient measurements in  $^{20}\text{Ne}$  and  $^{32}\text{S}$ .

This count demonstrates that the systematics is a useful working hypothesis. It is too new for assuming its validity without exceptions. There may be unknown selection rules or distortions. The states called “complementary” must not be considered to be predictions. Particularly, the validity of the systematics does not depend on the existence of the  $^{20}\text{Ne}$ , 0.688-MeV and  $^{32}\text{S}$ , 0.491-MeV levels.

The almost linear increase of the binding energy during the build-up of the  $1d_{5/2}$  subshell and the approximate parallelism of the three trends mean that the energy gain for the build-in of four  $1d_{5/2}$  nucleons is independent of the number of  $1d_{5/2}$  and  $1d_{3/2}$  nucleons already present.

When working with these diagrams, one should keep in mind that they contain the compensation term  $(9.5\text{ MeV}) \cdot A$ . This means that the level scheme of the next nuclide four mass units higher is shifted up as much as  $4 \times 9.5\text{ MeV} = 38\text{ MeV}$ . Therefore the difference between rising and falling trends is meaningless.

### 5. Enlarged View of the Almost Horizontal $0^+$ Trends

Figure 4 is the first of four diagrams which show the 14 almost straight trends in Fig. 3 on an extremely enlarged scale. The trends look like broken lines now, but they are still approximately linear. This figure displays the three almost horizontal trends of the lower parallelogram-like shape.

Instead of  $C = 9.5\text{ MeV}$  in the linear term of the quantity plotted, other constants are employed which normalize the three points on the right side of the trends. In each of the trends, the lower, middle, and upper trend, the data are incomplete. Therefore it is merely an assumption that these three points form an exactly straight line.

The other structure of Fig. 3, which also approximates

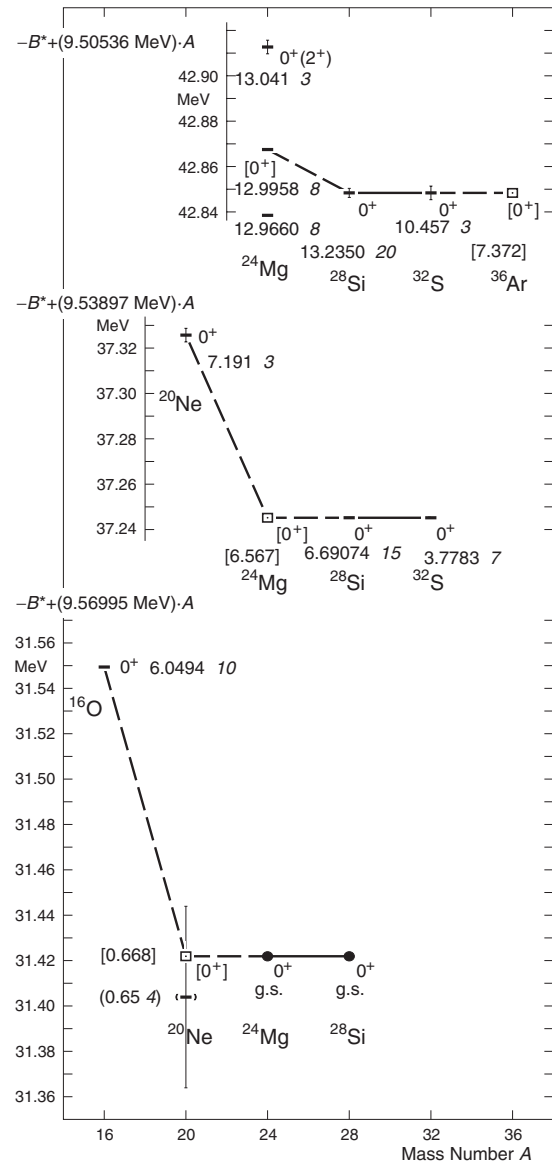


Fig. 4. Nearly horizontal trends of the lower parallelogram of Fig. 3. The vertical scale is tremendously enlarged, so that the unit shown is now 10 keV instead of 1 MeV. Therefore the “almost linear trends” show huge breaks. The exact straightness of the right part is merely an assumption (see text). Normalization of these three points leads to compensating factors other than 9.5 MeV. For the complementary levels (squares), the estimated uncertainty of 30 keV is not shown. See also captions in Figs. 1 and 2.

to a parallelogram and also consists of 6 small shapes approximating to parallelograms, is characterized by the presence of a  $2s_{1/2}$  subshell occupied by two protons and two neutrons. The lowest of the three trends was identified as such earlier.<sup>5)</sup> One of the three points on the right side is also missing in each trend.

Such a straight-line-assumption is suggested by the fact that the first  $2^+$  levels of  $^{20}\text{Ne}$ ,  $^{24}\text{Mg}$ , and  $^{28}\text{Si}$  form a trend<sup>5)</sup> which deviates, updated, by only 8 keV from linearity, so that the  $^{24}\text{Mg}$  level lies 4 keV below the connecting line of the other two levels. The straight-line-assumption is obviously an approximation within about 30 keV if the whole trend were actually smoothly curved. A break may be caused by the fact that the points on the left side correspond to an empty subshell in contrast to one partly or completely filled.



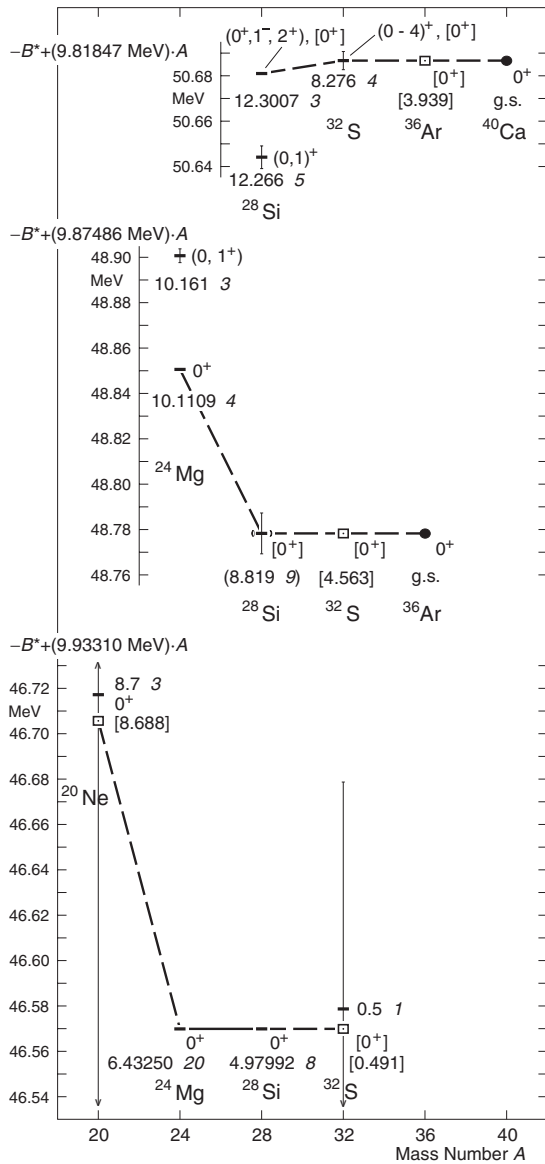


Fig. 5. Nearly horizontal trends of the higher parallelogram in Fig. 3. In the lower trend, the uncertainty of the known 8.7-MeV,  $0^+$  level is estimated to be 300 keV and therefore could not be shown. The level  $^{32}\text{S}$   $0.5 \pm 0.1$  MeV reported by Snowdon<sup>20)</sup> is shown without computing an average with the value 0.43 MeV reported by Singh,<sup>21)</sup> because he gave no uncertainty. Due to the limited empirical data, the use of a complementary value of 8.688 MeV instead of the experimental value 8.7 MeV was arbitrarily obtained by using the small break in the upper 4-point trend (of which the connecting lines are not shown) in Fig. 6 for Fig. 7 below. See also caption in Figs. 1, 2, and 4.

Figure 5 presents the three declining trends of the higher, somewhat rotated, parallelogram-like shape of Fig. 3 in the same manner as in Fig. 4.

It is desirable also to enlarge the steep trends of Fig. 3 connecting three points each in order to see how straight these trends are.

### 6. Enlarged View of the Steep $0^+$ Trends

Figure 6 shows the steep trends on an extremely enlarged scale for the lower parallelogram-like shape of Fig. 3 which connects states with an empty  $2s_{1/2}$  subshell. They were already shown in Fig. 4 by grouping the almost horizontal trends.

It should be noted that the normalization of the second and third point of the steeply rising trends leads to declining trends. The interesting new information of Fig. 6 is that the sizes of the breaks are uniformly about 100 keV. This is only about a  $5 \times 10^{-4}$  or 0.05% deviation from a straight line in relation to the binding energy.

Figure 7 correspondingly presents the four steep trends of the higher parallelogram-like shape of Fig. 3 already shown in Fig. 5 in a different grouping.

The new information of Fig. 7 is that the deviations from a straight line are also uniformly about 100 keV as in Fig. 6.

### 7. Comparison of Two $0^+$ Trends in the Range $A = 8$ to $32$

Figure 8 shows how two of the trends can be extended to smaller mass numbers.

The states of the lower trend have an empty  $2s_{1/2}$  subshell and the ones of the upper trend have this subshell filled by 2 protons and 2 neutrons. One level of the upper trend is missing and was tentatively placed at 6.064 MeV in  $^{16}\text{O}$ , just 15 keV above the known 6.0494 MeV level. It should be  $^{12}\text{C}$  in its ground state with  $(2s_{1/2})^4$  attached. In this case, a cross indicates a reference point instead of a complementary level (square) because such a state could happen to coincide with the 6.049-MeV level. This puzzle was noted earlier.<sup>5)</sup>

### 8. Comparison of Rotational Bands

Figure 9 shows the bands of  $^{16}\text{O}$ ,  $^{20}\text{Ne}$ ,  $^{24}\text{Mg}$ , and  $^{28}\text{Si}$  up to spin  $6^+$  in the representation of  $-B^* + (9.5) \cdot A$  versus the mass number  $A$  explained above.

The  $2^+$  trend from  $^{20}\text{Ne}$  over  $^{24}\text{Mg}$  to  $^{28}\text{Si}$  differs, when updated, by only 8 keV from linearity, so that the  $^{24}\text{Mg}$  level lies 4 keV below the connecting line of the other two levels.

The figure suggests that the band-head in  $^{20}\text{Ne}$  lies at 0.65 MeV. The rotational diagram  $E_x$  versus  $J(J + 1)$ , where  $E_x$  is the excitation energy and  $J$  the nuclear spin, would then approximate much better to a straight line. This would imply that the last in-band gamma transition  $2^+ \rightarrow 0^+$  would be so weak that it did not show up in the past.

The same preference for the ground-state transition occurs in the superdeformed band of  $^{36}\text{Ar}$ ,<sup>25)</sup> where the last in-band transition to the band-head at 4.329 MeV was not seen. The supposed special structure of the ground states of  $^{20}\text{Ne}$  and  $^{32}\text{S}$  discussed above may enhance the ground-state transitions from the first  $2^+$  level.

### 9. Inclusion of Higher $2^+$ Levels

Figure 10 is a search for parallelogram-like structures as they were shown for  $0^+$  states in Fig. 3 above.

The upper halves of the two parallelogram-like figures are drawn with dotted lines, because at higher excitations many spin determinations are missing, the level density increases, and  $2^+$  levels may fractionate. It may be noted that a prolongation to  $^{40}\text{Ca}$  is not possible because of the doubly-magic nature of that nuclide, which excludes the existence of a low-lying  $2^+$  level.

### 10. Comparison of the Diagrams for $0^+$ and $2^+$ States

Figure 11 consists of the  $2^+$  levels of Fig. 10 which are

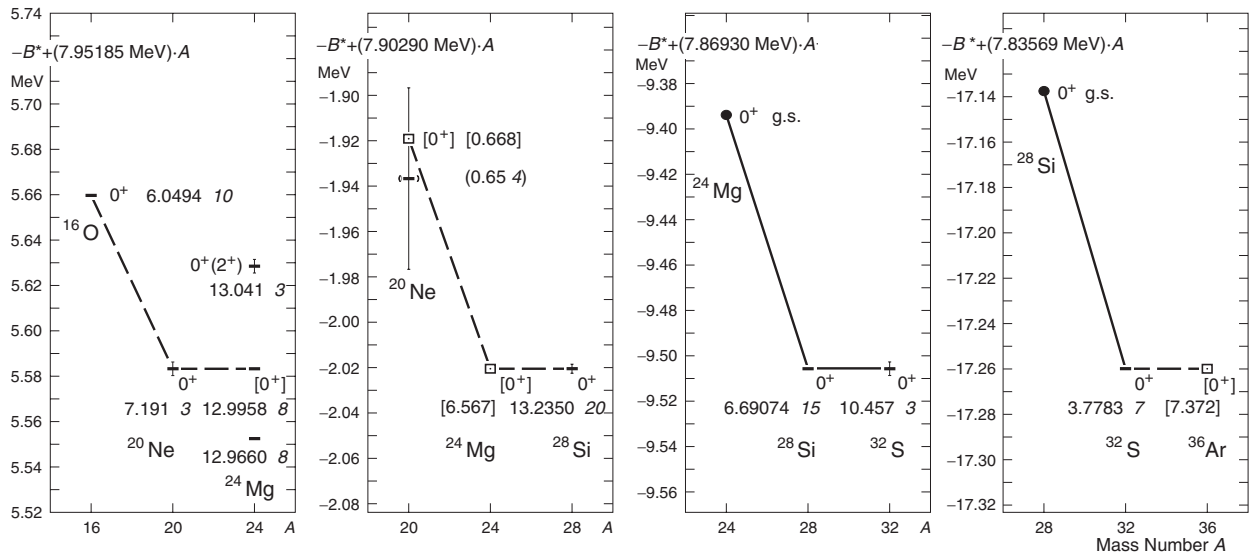


Fig. 6. Steep trends of the lower parallelogram of Fig. 2. The scale is enlarged as in Figs. 4 and 5. Normalization of the two points on the right leads to compensating factors other than 9.5 MeV which are equidistant for the second, third, and fourth part of this figure. Each of the four parts is adjusted so that the two points on the right are at the same height. For the policies regarding uncertainties, see the caption in Fig. 4. See also captions in Figs. 1 and 2.

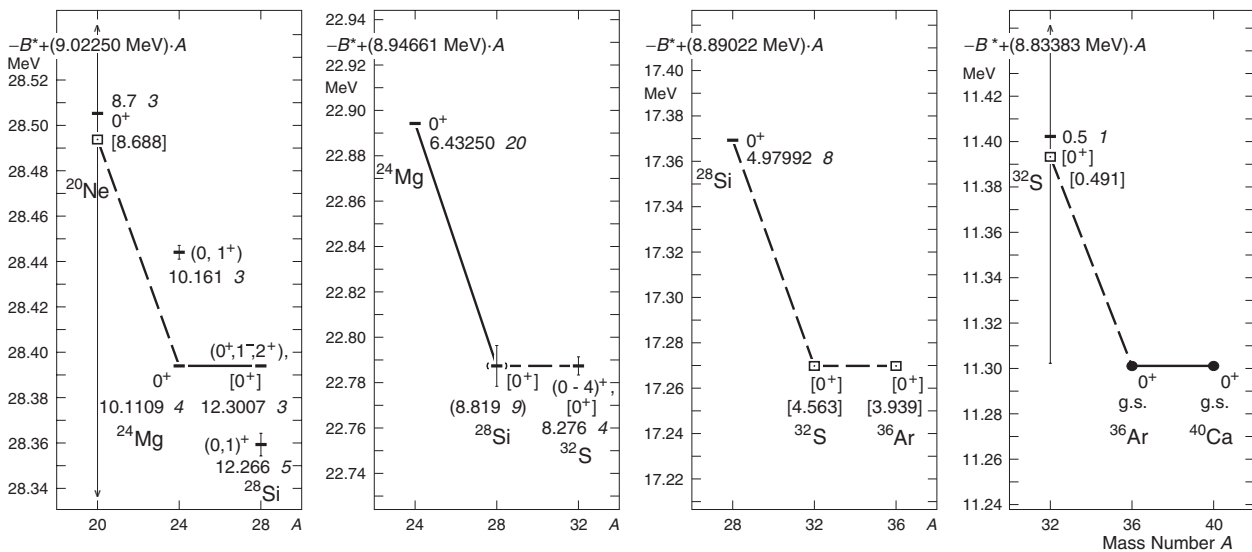


Fig. 7. Steep trends of the higher parallelogram in Fig. 3 corresponding to Fig. 6. See also explanation in Figs. 1, 2, and 6.

interconnected by lines, now drawn bold, and the two parallelogram-like shapes of Fig. 3 for spin  $0^+$ . The other  $2^+$  levels are omitted.

Should the band-heads in  $^{20}\text{Ne}$  and  $^{32}\text{S}$  really be the complementary levels indicated by squares, it is important that the ground states do not have their own  $2^+$  levels, in contrast to other  $0^+$  levels in this diagram. These ground states seem to have very special configurations, as already discussed above.

The other remarkable fact is that the  $0^+ \rightarrow 2^+$  excitations from  $^{20}\text{Ne}$  to the ground state of  $^{28}\text{Si}$  agree with the ones between the declining  $0^+$  and  $2^+$  trends from  $^{24}\text{Mg}$  to  $^{32}\text{S}$ . As discussed above, the second, declining set of  $0^+$  and  $2^+$  states has a  $2s_{1/2}$  subshell filled with 2 protons and 2 neutrons. This was previously shown in 1963,<sup>5)</sup> where the expected excitation energy of the missing  $^{28}\text{Si}$  level was

given as 6.31 10 MeV. Today, the expectation is almost unchanged at 6.308 30 MeV, 31.8 keV above a known  $3^+$  level at 6.27620 7 MeV, which may take away much strength in nuclear reactions.

Obviously, for the  $0^+ \rightarrow 2^+$  excitation energies it does not matter whether the  $2s_{1/2}$  subshell is occupied.

With two exceptions, the same is approximately true if the  $1d_{3/2}$  subshell of all members is occupied by 4 nucleons. This can be seen in the second 4-point trends (from below) of the lower and the slanted (“upper”) parallelogram-like figures. The first exception is caused by the fact that the pair of complementary levels (indicated by squares) at 7.308 MeV,  $2^+$  and 6.567 MeV,  $0^+$  in  $^{24}\text{Mg}$  has not been observed. The second exception relates to the pair of complementary levels 6.037 MeV,  $2^+$  and 4.563 MeV,  $0^+$  in  $^{32}\text{S}$ . If the  $0^+$  level is non-existent or very weakly populated, the same is

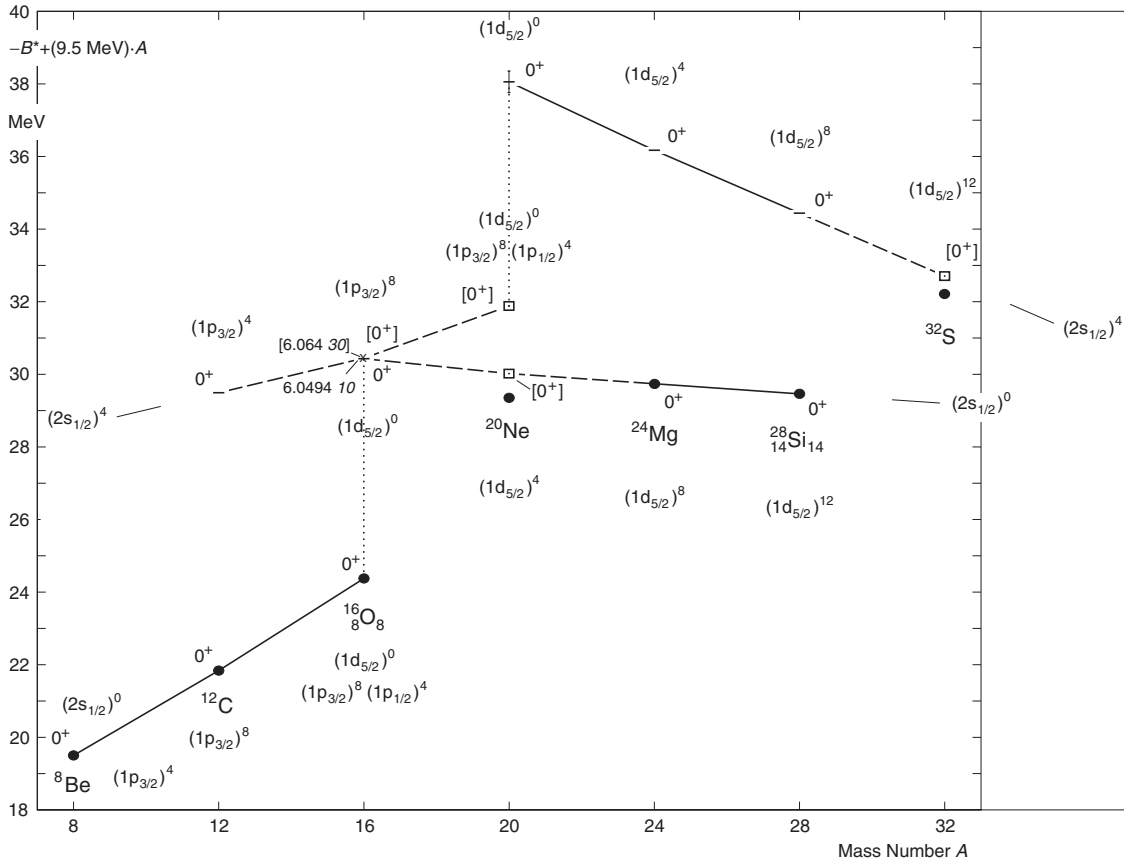


Fig. 8. Comparison of part of the trend of Fig. 1, for which the  $2s_{1/2}$  subshell is empty, with the trend in Fig. 2 and its extension to the  $0^+$  level of  $^{12}\text{C}$ , for which it is filled. Uncertainties are  $\leq 0.2$  keV unless indicated. See caption in Figs. 1 and 2.

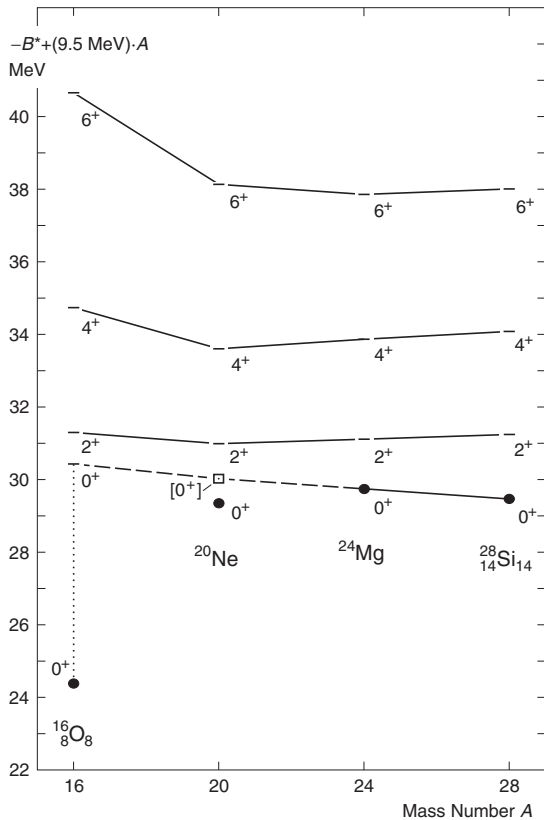


Fig. 9. Rotational bands up to  $6^+$  from  $^{16}\text{O}$  to  $^{28}\text{Si}$ . Uncertainties are  $\leq 7$  keV. See captions in Figs. 1 and 2.

expected for the  $2^+$  level directly above. In  $^{28}\text{Si}$ , the  $2^+$  level at 6.308 MeV is missing although the 4.97992 MeV,  $0^+$  level is known. Therefore the chances that a very weak 6.308-MeV,  $2^+$  level exists are much greater than for the other two  $2^+$  levels.

Figure 12 shows the excellent agreement particularly for the lowest 4-point trends. The second 4-point trends differ systematically from each other between 200 and 262 keV from  $^{24}\text{Mg}$  to  $^{32}\text{S}$  and  $^{28}\text{Si}$  to  $^{36}\text{Ar}$ , respectively.

The low point on the left side of the left diagram is the difference of the  $2^+$  level at 9.0018 MeV and the  $0^+$  level at 8.73 MeV, yielding 0.33 MeV. The uncertainty of the level reported at  $\approx 8.7$  MeV is estimated by the author. The low position of the difference depends on the assignment of the 9.00-MeV,  $2^+$  level as belonging to the band-head at 8.7 MeV, which leads to a strong deviation of the plot  $E_x$  versus  $J(J+1)$  from linearity.

### 11. Diagram of $J^\pi = 3^-$ and $4^-$ , $T = 0$ States for $A = 16$ to $40$

Figure 13 includes all  $3^-$  and  $4^-$ ,  $T = 0$  levels for the even-even self-conjugate nuclides from  $^{16}\text{O}$  to  $^{40}\text{Ca}$  up to the height indicated by 3 dots. All levels are omitted of which the spin and parity is not  $3^-$  or  $4^-$ ,  $T = 0$ . In  $^{20}\text{Ne}$ , also the levels at 5.621, 7.004, 7.156, and 10.406 MeV are omitted as they are known to be rotational  $3^-$ ,  $4^-$ ,  $3^-$ , and  $3^-$  levels with  $K^\pi = 2^-, 2^-, 0^-,$  and  $1^-$ . If no assignment exists for a level, it is included, because it may turn out to have one of these spins. Shell model configurations are indicated on the trends.



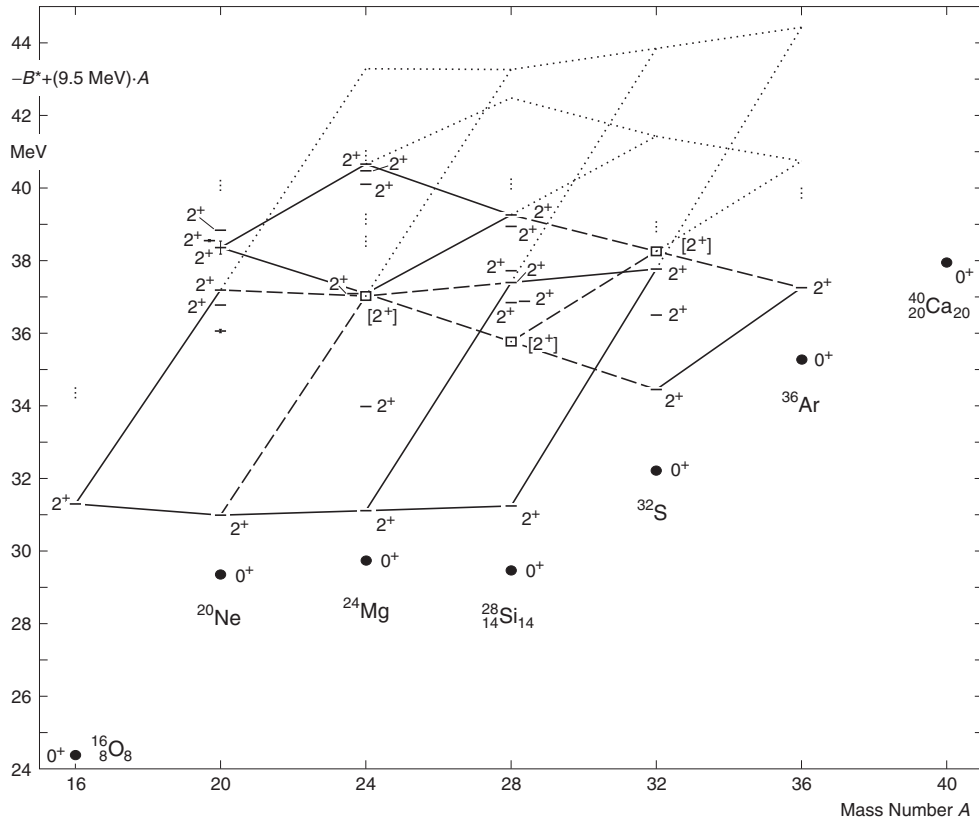


Fig. 10. Binding-energy diagram as in Fig. 2, but for established, possible, and complementary  $2^+$ ,  $T = 0$  levels. The complementary level (square) at 7.308 30 MeV in  $^{24}\text{Mg}$  belongs to the nearly horizontal dashed line. Slightly higher, there is a known  $2^+$  level which belongs to the declining trend. Uncertainties are  $\leq 3 \text{ keV}$  unless indicated. See also caption in Figs. 1 and 2.

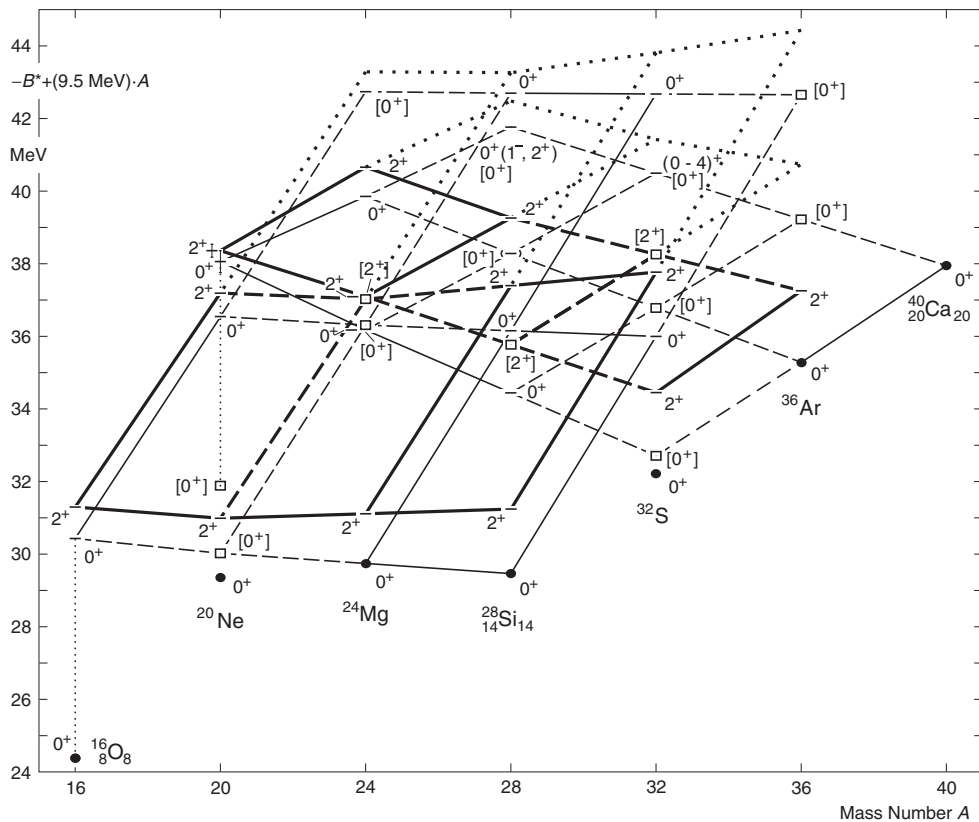


Fig. 11. Points with spin  $2^+$  which are situated on the two structures approximating to parallelograms (with a corner missing at  $^{40}\text{Ca}$ ) in Fig. 10, drawn with heavy lines, together with those of spin  $0^+$  from Fig. 3. See also caption in Figs. 1 and 2.

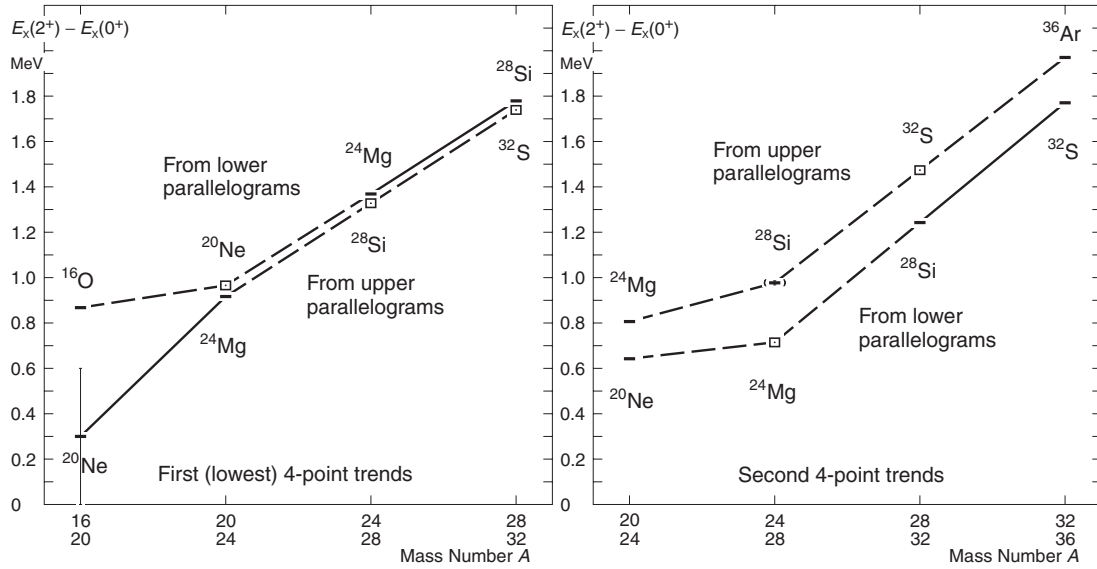


Fig. 12. Differences of excitation energies  $E_x(2^+) - E_x(0^+)$ . Uncertainties are  $\leq 3$  keV unless indicated. The squares in the differences occur if at least one term is complementary. In these cases each term has an estimated uncertainty of 30 keV (not shown). See also caption in Fig. 2.

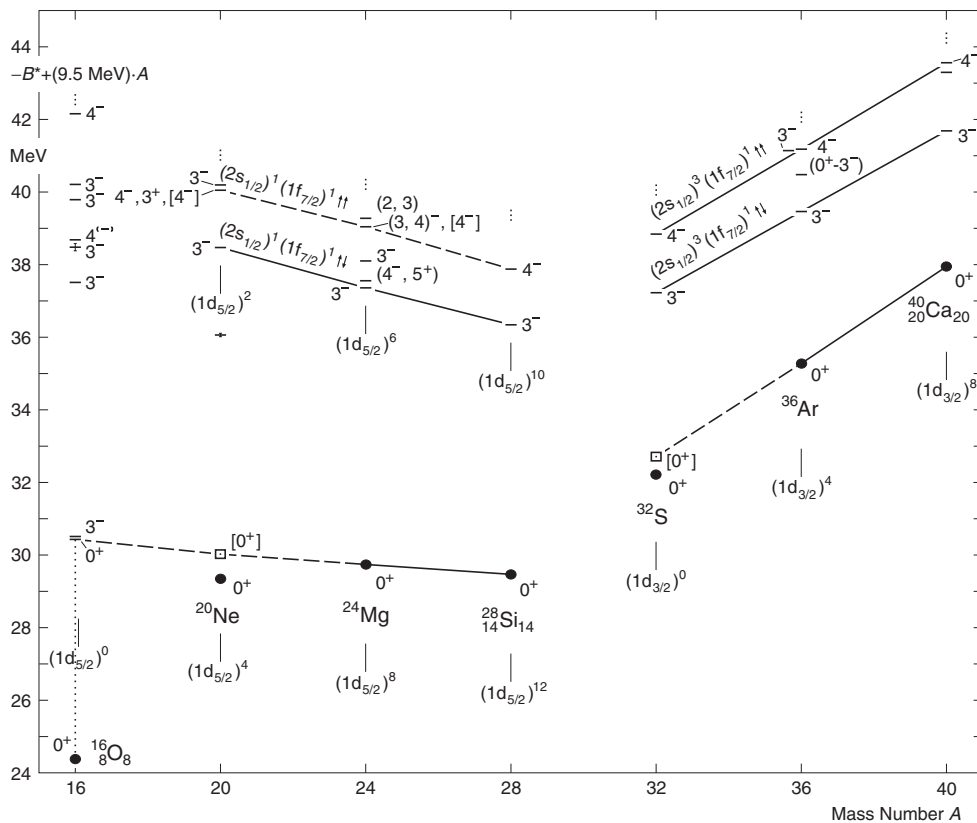


Fig. 13. Binding-energy diagram with the basic trend (see Fig. 2) and  $3^-$  and  $4^-$ ,  $T = 0$  states. Four rotational levels in  $^{20}\text{Ne}$  are omitted (see text).  $T = 0$  is omitted on all levels. Uncertainties are  $\leq 20$  keV unless indicated.

From  $^{20}\text{Ne}$  to  $^{28}\text{Si}$ , the supposed configurations  $(1d_{5/2})^2(2s_{1/2})^1(1f_{7/2})^1\uparrow\downarrow$ ,  $(1d_{5/2})^6(2s_{1/2})^1(1f_{7/2})^1\uparrow\downarrow$ , and  $(1d_{5/2})^{10}(2s_{1/2})^1(1f_{7/2})^1\uparrow\downarrow$  represent the build-up of the  $1d_{5/2}$  subshell. Approximately parallel and  $\approx 1.6$  MeV above there is a corresponding trend with possible  $4^-$  assignments which is interpreted as made up of the same configurations, but with parallel spins of the odd proton and neutron.

From  $^{32}\text{S}$  to  $^{40}\text{Ca}$ , a similar  $3^-$  trend with supposed

configurations  $(1d_{3/2})^0(2s_{1/2})^3(1f_{7/2})^1\uparrow\downarrow$ ,  $(1d_{3/2})^4(2s_{1/2})^3(1f_{7/2})^1\uparrow\downarrow$ , and  $(1d_{3/2})^8(2s_{1/2})^3(1f_{7/2})^1\uparrow\downarrow$  occurs, correspondingly with an approximately parallel  $4^-$  trend  $\approx 1.7$  MeV above with parallel spins.

The interpretation of the  $3^-$  and  $4^-$ ,  $T = 0$  levels is that a pair  $(1d_{5/2})^2\uparrow\downarrow$  is broken up and replaced by a coupling of a  $2s_{1/2}$  with a  $1f_{7/2}$  nucleon antiparallel to result in  $3^-$  and parallel to result in  $4^-$ . The odd proton and neutron are

understood as being indistinguishable, so that it is undetermined which one is in the  $1f_{7/2}$  state. This is in agreement with the fact that there is only *one*  $3^-$  and  $4^-$  level in each case instead of two.

It is easy to understand why the trends do not start at  $^{16}\text{O}$ : there is no pair  $(1d_{5/2})^2 \uparrow\downarrow$  available which could be broken apart.

The systematics involves 12 levels of which 10 have the suitable spin, while in  $^{20}\text{Ne}$  an expected  $4^-$  level has an assignment of  $4^-, 3^+$  and in  $^{24}\text{Mg}$  an expected  $4^-$  level has an  $(3, 4)^-$  assignment.

### 12. Discussion of the Almost Linear Trends

In the preceding figures, 22 mostly tentative nearly linear trends concerning the binding energy of nuclear states were shown. As mentioned in the introduction, the first examples of linear relations date back to 1958.<sup>4)</sup> At that time their number was only 8 and the low precision allowed exactly straight lines to be drawn within the uncertainties. Today, the expected deviations from linearity are well established and many more trends are known. Many of them have a gradually increasing slope with increasing mass number.

A recent investigation of mirror nuclides led to the hypothesis that the protons accommodated in a subshell are evenly distributed there, independent of their number.<sup>26)</sup> If this applies to nucleons in general, the two-body nuclear interaction with nucleons in other subshells would result in a linear trend, while these interactions within a subshell would

increase more than linearly. The same situation applies to the Coulomb repulsion of the protons. These two opposite effects apparently almost compensate each other in this mass region with the result of almost linear trends. In the  $1f_{7/2}$  subshell beyond  $^{40}\text{Ca}$ , however, the trends are generally bent upward by more than 100 keV per four mass units, due to a dominating Coulomb repulsion.

### 13. Discussion of Steps

As is obvious from Fig. 1, self-conjugate nuclides show steps at the doubly magic  $^4\text{He}$ ,  $^{16}\text{O}$ , and  $^{40}\text{Ca}$  only, but not at the doubly semi-magic  $^{28}\text{Si}$  and the doubly magic  $^{56}\text{Ni}$ . *Breaks* instead of steps occur there, as is expected when a new subshell with a smaller gain in energy is occupied by the incorporation of two protons and two neutrons once or several times. The slope increases at the break as would be expected in a diagram of, essentially, the negative binding energy.

It is known that there are two kinds of magic numbers; *the distinction agrees with the difference between steps and breaks*.

The observed magic numbers—given in bold face below—come from the two sequences, namely (a) the isotropic harmonic oscillator shell closures, and (b) the modified sequence given below. The less-pronounced semi-magic numbers for  $N$  or  $Z$  equal to 14 and 40 (not to be confused with  $A = 40$  at  $^{40}\text{Ca}$  with  $N = Z = 20$ ) are given in parentheses.

	(a)		<b><math>N</math> or <math>Z =</math></b>	<b>2</b>	<b>8</b>	<b>20</b>	<b>(40)</b>	70	112
			Subshell occupation numbers added:	4	6	8	10	12	14
	(b)		<b><math>N</math> or <math>Z =</math></b>	<b>6</b>	<b>(14)</b>	<b>28</b>	<b>50</b>	<b>82</b>	<b>126</b>

Figure 1 has shown that steps occur only at magic numbers of series (a) for  $N$  and  $Z = 2, 8,$  and  $20$  (or  $A = 4, 16,$  and  $40$  since  $N = Z$  and  $A = N + Z$ ), but not at the semi-magic or magic numbers of series (b) for  $N$  or  $Z = 14$  and  $28$  (or  $A = 28$  and  $56$ ).

The masses of self-conjugate even–even nuclides directly above  $^{80}\text{Zr}_{40}$  are not yet known; this makes the search for a step at  $A = 80$  impossible. However, evidence of irregularities for nuclides with  $N - Z > 0$  in that region was already obtained in 1964.<sup>27)</sup>

Figure 1 has shown that after the steps at  $^4\text{He}$ ,  $^{16}\text{O}$ , and  $^{40}\text{Ca}$ , the slope of the trend *decreases*. However, the well-known single-particle level representation requires a break with a subsequently *larger* slope as seen in the case of  $^{28}\text{Si}$  and  $^{56}\text{Ni}$ .

This was the second reason (besides the step itself) to explain the step phenomenon as a nucleon *rearrangement needed to accommodate the next subshell* in a regular way. The rearrangement defines a new lower slope independent of the previous one.

### 14. Suggested Experimental Clarifications

Table I below shows 18 desirable experimental clarifications.

The fact that 7 complementary levels (and one reference point from Fig. 8, no. 1 in the table) of spin  $0^+$  have not been detected and an additional 3 were detected only with

old methods, may be due to extremely weak population or neglect of parentage requirements. It should be noted that, e.g., the established  $^{20}\text{Ne}$  8.7-MeV  $0^+$  level was *only observed in one reaction*,  $^{16}\text{O}(\alpha, \alpha)$ , but not in the other reactions investigated leading to  $^{20}\text{Ne}$ . There is the *huge number of 74*, of which those reactions covering this excitation energy should be considered. In this case, the width is  $\Gamma_{\text{cm}} > 800$  keV, which makes the detection and a determination of the excitation energy difficult.

This example shows that the non-existence of a level cannot be proven by pointing to the large number of investigations in which the level did not appear. The reaction must be selected with respect to parentage considerations and the search has to concentrate on the expected energy range to ensure good statistics.

A scientifically correct way, after the levels had been reported, would be to set an upper limit on their population using modern equipment. This has not been done yet; the three papers<sup>18,20,21)</sup> were not mentioned in subsequent studies employing the original (d,n) reaction and the reaction ( $^3\text{He}, d$ ). From the viewpoint of parentage, there are more promising reactions, such as  $^{24}\text{Mg}(d, ^6\text{Li})^{20}\text{Ne}$ , to arrive at the suspected pure configuration  $(1d_{5/2})^4$  in  $^{20}\text{Ne}$ , and  $^{36}\text{Ar}(d, ^6\text{Li})^{32}\text{S}$  to arrive at  $(2s_{1/2})^4$ .

$E0$  transitions should be re-examined for possible populations of the low-lying  $0^+$  levels in question. The  $\gamma$ -decay of the lowest  $2^+$  levels of  $^{20}\text{Ne}$  and  $^{32}\text{S}$  may be studied if the

Table I. Reference points, complementary levels, and requirements for known levels.

Number	Nuclide	$E_x$ (MeV) required	$J^\pi; T$ required	$E_x$ (MeV) experimental	$J^\pi; T$ experimental	Figures	Ref.
1	$^{16}\text{O}$	6.064 30 reference point	$0^+; 0$	—	—	2, 8	—
2	$^{20}\text{Ne}$	0.668 30	$0^+; 0$	(0.65 4) <sup>a)</sup>	—	2, 3, 4, 6, 8, 9, 11, 13	18
3	$^{20}\text{Ne}$	as observed	$0^+; 0$	(2.53 7) <sup>a)</sup>	—	2, 3, 8, 11	18
4	$^{20}\text{Ne}$	8.688 30	$0^+; 0$	8.7 3 <sup>b)</sup>	$0^+; 0$	2, 3, 5, 7, 8, 11	14
5	$^{20}\text{Ne}$	as observed	$4^-; 0$	10.694 6	$4^-, 3^+; 0$	13	14
6	$^{24}\text{Mg}$	6.567 30	$0^+; 0$	—	—	2, 3, 4, 6, 11	—
7	$^{24}\text{Mg}$	7.308 30 <sup>c)</sup>	$2^+; 0$	—	—	10, 11	—
8	$^{24}\text{Mg}$	as observed	$4^-; 0$	9.2998 3	$(3, 4)^-; 0$	13	15
9	$^{24}\text{Mg}$	as observed	$0^+; 0$	12.9958 8	—	2, 3, 4, 6, 11	15
10	$^{28}\text{Si}$	6.308 30 <sup>d)</sup>	$2^+; 0$	—	—	10, 11	—
11	$^{28}\text{Si}$	as observed	$0^+; 0$	(8.819 9)	—	2, 3, 5, 7, 11	15
12	$^{28}\text{Si}$	as observed	$0^+; 0$	12.3007 3	$0^+(1^-, 2^+); 0 + 1^e)$	2, 3, 5, 7, 11	15
13	$^{32}\text{S}$	0.491 30	$0^+; 0$	0.5 1 <sup>a)</sup> and 0.43 <sup>a)</sup>	—	2, 3, 5, 7, 8, 11	20, 21
14	$^{32}\text{S}$	4.563 30	$0^+; 0$	—	—	2, 3, 5, 7, 11	—
15	$^{32}\text{S}$	6.037 30 <sup>f)</sup>	$2^+; 0$	—	—	10, 11	—
16	$^{32}\text{S}$	as observed	$0^+; 0$	8.276 4	$(0-4)^+; 0$	2, 3, 5, 7, 11	15
17	$^{36}\text{Ar}$	3.939 30	$0^+; 0$	—	—	2, 3, 5, 7, 11	—
18	$^{36}\text{Ar}$	7.372 30	$0^+; 0$	—	—	2, 3, 4, 6, 11	—

a) Insufficient evidence, omitted in compilations.

b) Uncertainty estimated by the present author. More precise energy desired, but  $\Gamma_{\text{c.m.}} > 800$  keV.

c) On the second 4-point trend (from below) of the lower parallelogram-like shape in Fig. 10.

d) On the first (lowest) 4-point trend of the upper parallelogram-like shape in Fig. 10. The agreement of decimals with no. 7 is accidental.

e)  $T$ -value not shown in Figs. 2, 3, 5, 7, and 11.

f) On the second 4-point trend (from below) of the upper parallelogram-like shape in Fig. 10.

Compton background can be sufficiently reduced. For both  $^{20}\text{Ne}$  and  $^{32}\text{S}$ , proton inelastic scattering experiments may also be tried in a search for the low-lying  $0^+$  states.

It should be noted that Morita and Takeshita<sup>18)</sup> reported not just one, but *two* doubtful levels (0.65 and 2.53 MeV), both of which fit the systematics excellently as already noticed in 1963.<sup>5)</sup> The idea that *both* measurements are erroneous is so *extremely remote* that an elaborate experimental clarification with present techniques is certainly worthwhile and overdue.

The reaction  $^{19}\text{F}(d,n)^{20}\text{Ne}$  was repeated as *test runs* in 1999 by K. Baba of Tohoku University at Sendai, Japan<sup>28)</sup> and in 2000 by J. Rapaport of Ohio University at Athens, Ohio, U.S.A.<sup>29)</sup> Both test runs showed that the sizes of the peaks drawn in the original paper<sup>18)</sup> in relation to the ground state yield were larger than those of the statistical fluctua-

tions observed now. In both cases, the preliminary work was discontinued without the further effort necessary to improve the statistics. In view of the arguments above, a search for a very weak population of the two levels in  $^{20}\text{Ne}$  reported in 1958<sup>18)</sup> is still needed. Their absence must not be concluded on the basis of unpublished test runs.

Concerning spin  $2^+$ , the table lists three complementary levels, of which the one in  $^{28}\text{Si}$ , no. 10, was proposed earlier.<sup>5)</sup> This is the only one of the three for which the  $0^+$  level below, to which it belongs, is known. The other two, nos. 7 and 15 of the table, belong to the  $0^+$  levels no. 6 and 14 of the table, also not known. Should they be forbidden, one would certainly assume the same for the  $2^+$  levels.

Concerning spin  $4^-$ , the table shows two desirable experimental clarifications. In addition, within the energy range shown in Fig. 13, there are 3 spins presently known

to be (2, 3), (4<sup>-</sup>, 5<sup>+</sup>) and (0<sup>+</sup>-3<sup>-</sup>). Their determination would improve the diagram if they happen not to be 3<sup>-</sup> or 4<sup>-</sup>.

Experimenters planning to work on items of the table are invited to contact the author to avoid a duplication of effort.

## 15. Conclusions

The nuclear binding-energy diagrams for spin 0<sup>+</sup>, Figs. 1–8, lead to partly established consistent patterns made up of almost linear trends connecting supposed approximately pure subshell states. For some complementary states and one reference point it is not sure whether they are forbidden by as yet unknown selection rules.

According to the systematics, the energy gain for the build-in of four 1d<sub>5/2</sub> nucleons is nearly independent of the number of 1d<sub>5/2</sub> and 1d<sub>3/2</sub> nucleons already there.

Trends in the nuclear binding energy for some rotational levels, more meaningful than the customary comparison by normalising the ground states, raise the question of whether the head of the lowest band in <sup>20</sup>Ne could lie at 0.668 MeV instead of being the ground state, thus supporting the complementary level of the 0<sup>+</sup> systematics.

The 2<sup>+</sup> levels from <sup>16</sup>O to <sup>36</sup>Ar form a system of parallelogram-like figures as the 0<sup>+</sup> states and therefore support these findings, particularly the complementary level at 0.491 MeV in <sup>32</sup>S.

The energies of 2<sup>+</sup> excitations above 0<sup>+</sup> states approximately agree with each other for two pairs of trends. The excitation energies are independent of the occupation of the 2s<sub>1/2</sub> subshell and approximately independent of the occupation of the 1d<sub>3/2</sub> subshell by 4 nucleons.

For the 3<sup>-</sup> and 4<sup>-</sup> levels, the binding-energy diagram leads to two pairs of approximately linear and parallel trends connecting supposed approximately pure subshell states. They suggest that not only the energy gain for the build-in of four 1d<sub>5/2</sub> nucleons is independent of the number of 1d<sub>5/2</sub> nucleons already present (like for the 0<sup>+</sup> states), but also the “spin-flip” energy between the 4<sup>-</sup> and 3<sup>-</sup> levels.

The nearly linear 3<sup>-</sup> and 4<sup>-</sup> trends support the expectation that the two 0<sup>+</sup> trends below, defined by the ground states of <sup>24</sup>Mg and <sup>28</sup>Si as well as <sup>36</sup>Ar and <sup>40</sup>Ca, are also linear. This would support the other complementary 0<sup>+</sup> level in <sup>32</sup>S at 0.491 MeV already mentioned in addition to the one in <sup>20</sup>Ne at 0.668 MeV.

The near-linearity of the 3<sup>-</sup> and 4<sup>-</sup> trends is a new additional argument suggesting an experimental search for the two 0<sup>+</sup> levels in <sup>20</sup>Ne and <sup>32</sup>S.

It should be noted that an investigation of the *odd–odd* (instead of *even–even*) self-conjugate nuclides of spins 0<sup>+</sup>, *T* = 1 and 1<sup>+</sup>, 2<sup>+</sup>, and 3<sup>+</sup>, *T* = 0 from <sup>14</sup>N to <sup>38</sup>K<sup>30</sup> shows for the 99 nuclear states involved that the same subshell structure prevails. Particularly, the nuclide <sup>22</sup>Na is recognized by its large number of 9 reference points as having

an abnormal structure, obviously caused by a core of <sup>20</sup>Ne in its supposedly exceptional ground state.

- 1) F. Everling, L. A. König, J. H. E. Mattauch and A. H. Wapstra: Nucl. Phys. **25** (1961) 177.
- 2) F. Everling, L. A. König, J. H. E. Mattauch and A. H. Wapstra: 1960 Nuclear Data Tables (U.S. Government Printing Office, Washington, D.C., 1961) Part 1.
- 3) J. Mattauch and F. Everling: Prog. Nucl. Phys. **6** (1957) 233.
- 4) F. Everling: Z. Naturforsch. A **13** (1958) 900.
- 5) F. Everling: Nucl. Phys. **40** (1963) 670.
- 6) F. Everling: Nucl. Phys. **47** (1963) 561.
- 7) F. Everling: Z. Naturforsch. A **14** (1959) 787.
- 8) F. Everling: Nucl. Phys. **36** (1962) 228.
- 9) F. Everling: Nucl. Phys. A **144** (1970) 539.
- 10) F. Everling: Nucl. Phys. A **115** (1968) 563.
- 11) G. Audi, A. H. Wapstra and C. Thibault: Nucl. Phys. A **729** (2003) 337.
- 12) F. Ajzenberg-Selove: Nucl. Phys. A **506** (1990) 1.
- 13) D. R. Tilley, H. R. Weller and C. M. Cheves: Nucl. Phys. A **564** (1993) 1.
- 14) D. R. Tilley, C. M. Cheves, J. H. Kelley, S. Raman and H. R. Weller: Nucl. Phys. A **636** (1998) 249.
- 15) P. M. Endt: Nucl. Phys. A **521** (1990) 1; supplemented by Nucl. Phys. A **633** (1998) 1.
- 16) J. A. Cameron and B. Singh: Nucl. Data Sheets **102** (2004) 293.
- 17) F. Everling: Int. Workshop PINGST 2000, Selected Topics on *N* = *Z* Nuclei, Lund, Sweden, ed. D. Rudolph and M. Hellström, Department of Physics, Lund University, S-22100 Lund, Sweden (2000) p. 204.
- 18) S. Morita and K. Takeshita: J. Phys. Soc. Jpn. **13** (1958) 1241.
- 19) A. N. Andreyev, M. Huyse, P. Van Duppen, L. Weissman, D. Ackermann, J. Gerl, F. P. Hessberger, S. Hofmann, A. Kleinböhl, G. Münzenberg, S. Reshitko, C. Schlegel, H. Schaffner, P. Cagarda, M. Matos, S. Saro, A. Keenan, C. Moore, C. D. O’Leary, R. D. Page, M. Taylor, H. Kettunen, M. Leino, A. Lavrentiev, R. Wyss and K. Heyde: Nature **405** (2000) 430.
- 20) S. C. Snowden: Phys. Rev. **87** (1952) 1022.
- 21) R. G. Singh: Ph. D. Thesis, University of Florida 1956; Diss. Abstr. 17 (1957) 386.
- 22) A. T. G. Ferguson, L. Nilsson and N. Starfelt: Nucl. Phys. A **111** (1968) 423.
- 23) F. Everling: Z. Naturforsch. A **15** (1960) 84.
- 24) F. Everling, G. L. Morgan, D. W. Miller, L. W. Seagondollar and P. W. Tillman, Jr.: Can. J. Phys. **49** (1971) 402.
- 25) C. E. Svensson, A. O. Macchiavelli, A. Juodagalvis, A. Poves, I. Ragnarsson, S. Aberg, D. E. Appelbe, R. A. E. Austin, C. Baktash, G. C. Ball, M. P. Carpenter, E. Caurier, R. M. Clark, M. Cromaz, M. A. Deleplanque, R. M. Diamond, P. Fallon, M. Furlotti, A. Galindo-Uribarri, R. V. F. Janssens, G. J. Lane, I. Y. Lee, M. Lipoglavsek, F. Nowacki, S. D. Paul, D. C. Radford, D. G. Sarantites, D. Seweryniak, F. S. Stephens, V. Tomov, K. Vetter, D. Ward and C. H. Yu: Phys. Rev. Lett. **85** (2000) 2693.
- 26) F. Everling: in *Proc. Int. Conf. Exotic Nuclei and Atomic Masses, Bellaire, Michigan, U.S.A., 1998*, ed. B. M. Sherrill, D. J. Morrissey and C. N. Davids (American Institute of Physics, Woodbury, NY, 1998) p. 298.
- 27) F. Everling: in *Proc. Int. Conf. Phys., Paris, 1964*, ed. P. Gugenberger (Éditions du Centre National de la Recherche Scientifique, Paris, 1964) Vol. II, p. 447.
- 28) K. Ishii for M. Baba: private communication (1999).
- 29) J. Rapaport: private communication (2000).
- 30) F. Everling: in preparation for publication.